

Supplementary Materials

Type III and IV deformation twins in minerals and metals

John P. Hirth^{a,1,2}, Greg Hirth^b, and Jian Wang^{c,1}

^a Private address, Green Valley, AZ 54614; ^b Department of Geological Sciences, Brown University, Providence, RI 02912; and ^c Department of Mechanical and Materials Engineering, University of Nebraska–Lincoln, Lincoln, NE 68588. ¹To whom correspondence may be addressed. Email: jianwang@unl.edu or jphmdh8@gmail.com. ² Retired.

Appendix A. Matrix description of the twin in the TM

For a type I twin or a precursor to type II, the following conditions are true:

(A) P is an even-fold axis, most often $2'$.

(B) The t vectors that define the twin must lie in the plane of distortion, so that their projections in the twin plane are parallel to b .

A corollary is:

(C) If (B) is satisfied, then the glide plane is a mirror plane, normal to P .

These conditions ensure that a low index direction lies in the K_2 plane as specified in the classical theory. These conditions are always met in cubic crystals, and for most twins in tetragonal, orthorhombic crystals, and hexagonal crystals. Most twins in triclinic crystals and some twins in monoclinic and trigonal systems do not satisfy these requirements. The twins are then type III or provide a precursor to type IV. All the twin examples in the topological theory (TT) [13, 29], the basis for the TM, are for high symmetry crystals where Q is also a $2'$ axis. This implies that this is always true, but it is not for triclinic crystals, for example. Of course, the application of the TT to the triclinic case should give the same results as described here.

For a type III twin or a precursor to Type IV, (B) and (C) are not fulfilled and the following condition applies to P .

(D) P is an even-fold inversion axis, most often $\bar{2}'$.

We now outline the general procedure and demonstrate the twin symmetry for low symmetry crystals, following [7, 8]. In the TT and TM, there must be coherent terrace plane, here the twin plane. With the

composition plane coherent (and the nearby twin plane in the DP), one selects a commensurate site in the DP as the origin. The displacements in the twin are related to the matrix by

$$\mathbf{u} = \mathbf{D}\mathbf{t}_M \quad (\text{A1})$$

where \mathbf{D} is the distortion matrix $\nabla\mathbf{u}$. Then the translation vectors in the two lattices are related by

$$\mathbf{t}_T = \mathbf{t}_M + \mathbf{u} = (\mathbf{I} + \mathbf{D})\mathbf{t}_M \quad (\text{A2})$$

In the TT, for a unit TD, $\mathbf{u} = \mathbf{b}$ and

$$\mathbf{b} = \mathbf{t}_T - \mathbf{M}\mathbf{t}_M \quad (\text{A3})$$

where \mathbf{M} is a coordinate transformation matrix, re-expressing \mathbf{t}_M in the twin frame. Here, as for Figure 2 in the text, \mathbf{M} can be an engineering shear or an interface rotation. Alternatively, as in [13], one can introduce a Burgers circuit into the DP to define \mathbf{b} , and the reduced circuit is defined by the origin, \mathbf{t}_T and \mathbf{t}_M . Thus, in a common DP frame, $\mathbf{b} = \mathbf{t}_T - \mathbf{t}_M$, Eq. (1). The twin plane remains coherent for the twin, so the same configuration is repeated for any three-site arrangement in the coherent plane. Therefore, the normal to the twin plane must be either a $\mathbf{2}'$ or a $\bar{\mathbf{2}}'$ axis. Hence the low index directions \mathbf{t}_T and \mathbf{t}_M have 2 or mirror local symmetry relative to the \mathbf{t}_0 vector of the same indices in a single crystal matrix as shown in Figure A1(a). The two \mathbf{t} vectors and their origin \mathbf{o} define a repeatable pair of planar triangles in the DP. The problem regarding symmetry for type III twins is that this plane is slanted relative to \mathbf{P} , which is therefore irrational. As in the text, the plane of distortion plane and the twinning angle α are defined by the *projections* of the translation vectors onto the plane of distortion. With the relevant three entities \mathbf{o}' , \mathbf{t}_{Tp} , and \mathbf{t}_{Mp} , the Burgers vector is given by

$$\mathbf{b} = \mathbf{t}_{Tp} - \mathbf{t}_{Mp} \quad (\text{A4})$$

and \mathbf{b} is the same as in Eq. (1). In the coherent twin plane, all sites have this triangular configuration, see Figure A1(a). If the \mathbf{t} vectors do not lie in the plane of distortion, as in Figures 3(d-f) there is no possible $\mathbf{2}'$ axis other than \mathbf{P} , which is irrational, and no possible \mathbf{m}' plane.

We now analyze type I planes in triclinic crystals. Figure A1(b) is a view parallel to the triangles in the glide plane in the DP in a triclinic crystal. This example, which differs from the classical type II case, is the only possible type II twin. As shown, \mathbf{n} is then irrational, being rotated by β from the nearest low-index, rational direction. $\mathbf{Q} // \mathbf{b}$ is not a $\mathbf{2}'$ axis because site B does not rotate to site A. Similarly, \mathbf{n} is not a $\mathbf{2}'$ axis, because sites A and B rotate to empty sites. Obviously, the same would be true if \mathbf{Q} were

irrational. Since the configuration at B is repeated at A after rotation, P is a $2'$ axis. Also, the double triangles at all lattice points in the glide planes have m' symmetry. Thus, for type I twins in triclinic crystals, conditions (A) to (C) are satisfied, but there are no $2'$ axes other than P .

The analog for type III is shown in Figure A1(c). P is now a $\bar{2}'$ axis. Site A rotates to B but the triangle is not the same as that at D, so it inverts back to C. Similarly, the t vectors above the glide plane are not mirror images of those below so there is no m' symmetry. Instead, the added symmetry is a glide-mirror plane, (m', p'_n) [44]. The *projected* translation vectors t_p and the displacement vectors b have $2'$ and m' symmetry but the DP has $\bar{2}'$ and (m', p'_n) symmetry only. Most rigid displacements, p , are associated with local relaxation at the interface, usually unknown. The offset in Figure A1(c) differs, but can be treated as a rigid shift p'_n parallel to n . All earlier work applying the TM dealt with high symmetry crystals and could imply that $2'$ and m' symmetry applied generally. However, Figure A1 proves that such is not the case for triclinic and some other lower symmetry lattices.

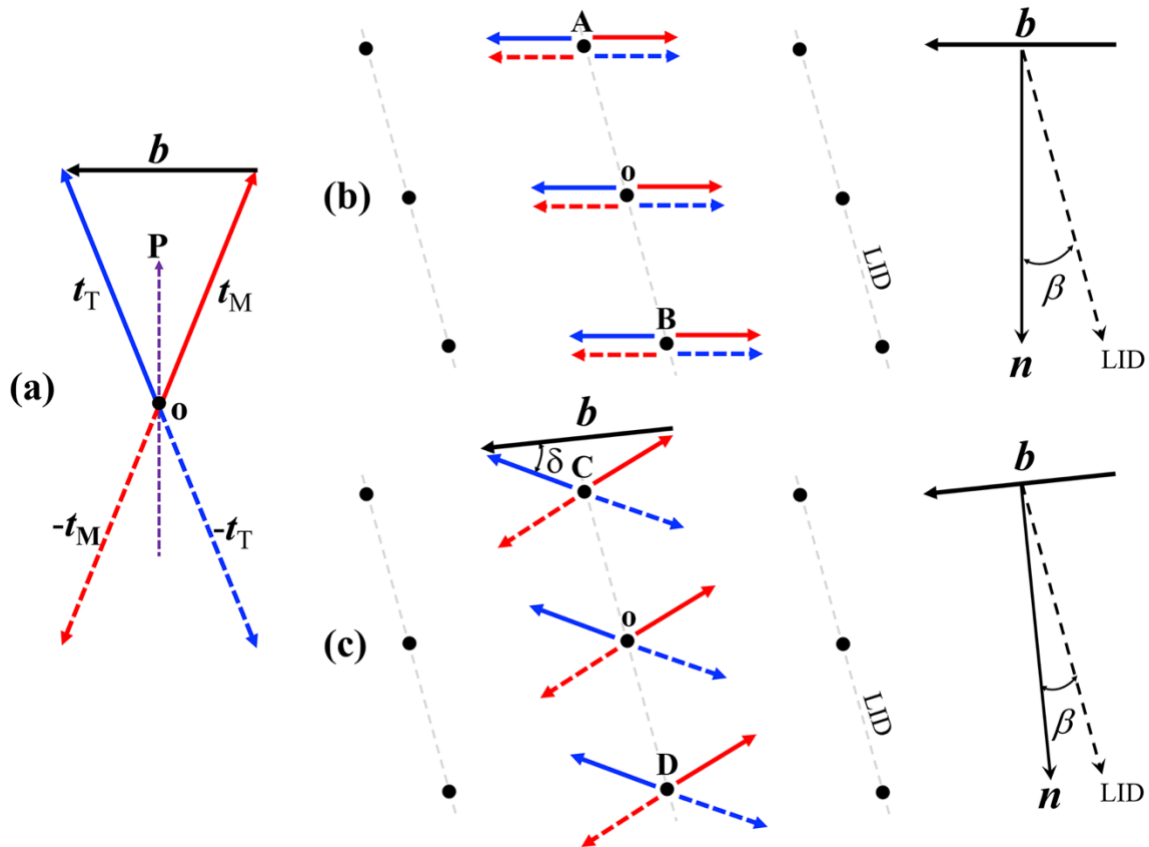


Figure A1. (a). View of double triangle formed by o , $\pm t_M$, and $\pm t_T$. (b). View of the glide plane of a type II twin in a triclinic crystal, also with a projection along n . (c). analog for a type III twin.

Appendix B: Twin characteristics for various compositions of plagioclase.

While the text treats the twinning of labradorite, we present data for various compositions of plagioclase. These indicate the regular trends in properties as a function of composition. The type-distinguishing parameter is zero for a labradorite and increases to maxima for albite and anorthite. The maximum value of δ is 33° and this corresponds to a difference in α values of 1.39° . Hence, the changes associated with the present work are significant. Determination of crystallographic quantities of twinning elements can be found in Supplementary Materials.

Table 1. Lattice parameters of plagioclase [32]. The lattice parameters vary continuously with composition; these are theoretical values for typical values in the middle of the composition range for the plagioclase series. The exception is An52, featured here, with a composition determined by wave-length dispersive spectroscopy [11].

Component/Name		Lattice parameters					
		$a_0(\text{nm})$	$b_0(\text{nm})$	$c_0(\text{nm})$	$\alpha_0(^{\circ})$	$\beta_0(^{\circ})$	$\gamma_0(^{\circ})$
An0	Albite	0.814	1.278	0.716	94.190	116.610	87.680
An16	Oligoclase	0.815	1.282	0.714	93.965	116.475	88.631
An28	Oligoclase	0.817	1.285	0.712	93.630	116.400	89.460
An38	Andesine	0.815	1.283	0.710	93.620	116.210	89.700
An52	Labradorite	0.818	1.286	0.711	93.530	116.210	89.920
An66	Labradorite	0.818	1.287	0.711	93.570	116.030	90.370
An85	Bytownite	0.819	1.288	0.710	93.370	116.040	90.870
An100	Anorthite	0.817	1.287	0.708	93.113	115.913	91.261

Table 2. Properties of type I and II twins in plagioclase.

Component	K_1	x_1	K_2	x_2	n	$2\alpha(^{\circ})$	$\beta(^{\circ})$	$\delta(^{\circ})$	$h_0(\text{nm})$	$2 b_g (\text{nm})$
An0	(010)	[-0.015 0 0.123]	(-1 0 1.587)	[010]	[1 0 0.630]	8.44	33.38	0	0.638	0.094
An16	(010)	[0.014 0 0.131]	(-1 0 2.534)	[010]	[1 0 0.395]	7.98	20.08	0	0.639	0.089
An28	(010)	[0.037 0 0.133]	(-1 0 5.859)	[010]	[1 0 0.171]	7.65	8.13	0	0.641	0.086
An38	(010)	[0.044 0 0.137]	(-1 0 10.508)	[010]	[1 0 0.095]	7.80	4.42	0	0.640	0.087
An52	(010)	[0.050 0 0.137]	(-1 0 38.333)	[010]	[1 0 0.026]	7.80	1.18	0	0.642	0.087
An66	(010)	[0.066 0 0.146]	(1 0 8.374)	[010]	[1 0 -0.119]	8.34	5.09	0	0.642	0.094
An85	(010)	[0.080 0 0.147]	(1 0 3.356)	[010]	[1 0 -0.298]	8.54	11.77	0	0.642	0.096
An100	(010)	[0.089 0 0.144]	(1 0 2.138)	[010]	[1 0 -0.468]	8.53	17.21	0	0.642	0.096

Table 3. Properties of type III/IV twins in plagioclase (special case with $\beta = 0$).

Component	K_1	x_1	K_2	x_2	n	$2\alpha(^{\circ})$	$\beta(^{\circ})$	$\delta(^{\circ})$	$h_0(\text{nm})$	$2 b_g (\text{nm})$
An0	(010)	[0.048,0,0.123]	(001)	[-0.064,1,0]	[1 0 0]	7.05	0	33.38	0.638	0.079
An16	(010)	[0.051,0,0.131]	(001)	[-0.038,1,0]	[1 0 0]	7.50	0	20.08	0.639	0.084
An28	(010)	[0.052,0,0.133]	(001)	[-0.015,1,0]	[1 0 0]	7.57	0	8.13	0.641	0.085
An38	(010)	[0.053,0,0.137]	(001)	[-0.008,1,0]	[1 0 0]	7.78	0	4.42	0.640	0.087
An52	(010)	[0.053,0,0.137]	(001)	[-0.002,1,0]	[1 0 0]	7.79	0	1.18	0.642	0.087
An66	(010)	[0.056,0,0.146]	(001)	[0.010,1,0]	[1 0 0]	8.31	0	5.09	0.642	0.093
An85	(010)	[0.056,0,0.147]	(001)	[0.024,1,0]	[1 0 0]	8.36	0	11.77	0.642	0.094
An100	(010)	[0.054,0,0.144]	(001)	[0.035,1,0]	[1 0 0]	8.15	0	17.21	0.642	0.092

Appendix C: Crystallographic analysis

1. Determination of crystallographic quantities of twinning elements.

For a triclinic lattice, the unit cell is described by three base vectors \mathbf{a}_0 , \mathbf{b}_0 and \mathbf{c}_0 , and the angles α_0 , β_0 , and γ_0 between \mathbf{b}_0 and \mathbf{c}_0 , \mathbf{c}_0 and \mathbf{a}_0 , \mathbf{a}_0 and \mathbf{b}_0 , respectively. Since the three base vectors are non-orthogonal, all vector operations have to be transformed to Cartesian coordinates, and then back to crystal coordinates.

1.1 Conversion between crystal direction and vectors in Cartesian coordinates

In the Cartesian coordinate system, a_0 is the magnitude of \mathbf{a}_0 in the positive x-axis direction, b_0 is a positive y-axis component of the \mathbf{b}_0 , and c_0 is the positive z-axis component of the \mathbf{c}_0 . With these conditions, the basis vectors \mathbf{a}_i of the Cartesian coordinate system are expressed by the following equations.

$$\begin{aligned}\mathbf{a}_1 &= (a_0, 0, 0) \\ \mathbf{a}_2 &= (b_0 \cos(\gamma_0), b_0 \sin(\gamma_0), 0) \\ \mathbf{a}_3 &= (c_x, c_y, c_z)\end{aligned}\quad (1)$$

Where,

$$\begin{aligned}c_x &= c_0 \cos(\beta_0) \\ c_y &= c_0 \frac{\cos(\alpha_0) - \cos(\gamma_0) \cos(\beta_0)}{\sin(\gamma_0)} \\ c_z &= \frac{\Omega}{a_0 b_0 \sin(\gamma_0)}\end{aligned}\quad (2)$$

$$\Omega = a_0 b_0 c_0 \sqrt{1 - \cos^2(\alpha_0) - \cos^2(\beta_0) - \cos^2(\gamma_0) + 2 \cos(\alpha_0) \cos(\beta_0) \cos(\gamma_0)}$$

Ω is the volume of a unit cell. The indices in the crystal coordinate system $[uvw]$ are converted to a vector in Cartesian coordinates by the following expression. A is the transformation matrix between crystal coordinate and Cartesian coordinates.

$$[xyz] = [uvw] \begin{bmatrix} \mathbf{a}_1 \\ \mathbf{a}_2 \\ \mathbf{a}_3 \end{bmatrix} = [uvw]A \quad (3)$$

$$A = \begin{bmatrix} a_0 & 0 & 0 \\ b_0 \cos(\gamma_0) & b_0 \sin(\gamma_0) & 0 \\ c_0 \cos(\beta_0) & \frac{c_0 (\cos(\alpha_0) - \cos(\beta_0) \cos(\gamma_0))}{\sin(\gamma_0)} & \frac{\Omega}{a_0 b_0 \sin(\gamma_0)} \end{bmatrix} \quad (4)$$

1.2 Conversion between Miller indices and plane normal in Cartesian coordinates

Similarly, the indices of crystal planes (Miller indices) and normal vector of a plane are related by reciprocal lattice vectors \mathbf{b} . The reciprocal lattice vectors are determined from the basis vectors in Cartesian coordinates in real space.

$$\begin{aligned}\mathbf{c}_1 &= \frac{\mathbf{a}_2 \times \mathbf{a}_3}{\mathbf{a}_1 \cdot (\mathbf{a}_2 \times \mathbf{a}_3)} \\ \mathbf{c}_2 &= \frac{\mathbf{a}_3 \times \mathbf{a}_1}{\mathbf{a}_2 \cdot (\mathbf{a}_3 \times \mathbf{a}_1)} \\ \mathbf{c}_3 &= \frac{\mathbf{a}_1 \times \mathbf{a}_2}{\mathbf{a}_3 \cdot (\mathbf{a}_1 \times \mathbf{a}_2)}\end{aligned}\quad (5)$$

The normal vector $[xyz]$ of a plane can be related to the index of this plane (hkl) by the following equation. Therefore, B is the transformation matrix between the Miller index of a plane and its normal.

$$[xyz] = [hkl] \begin{bmatrix} \mathbf{c}_1 \\ \mathbf{c}_2 \\ \mathbf{c}_3 \end{bmatrix} = [hkl] B \quad (6)$$

$$B = \begin{bmatrix} \frac{1}{a_0} & -\frac{\cos(\gamma_0)}{a_0 \sin(\gamma_0)} & -\frac{b_0 c_0 (\cos(\beta_0) - \cos(\alpha_0) \cos(\gamma_0))}{\sin(\gamma_0) \Omega} \\ 0 & \frac{1}{b_0 \sin(\gamma_0)} & -\frac{a_0 c_0 (\cos(\alpha_0) - \cos(\beta_0) \cos(\gamma_0))}{\sin(\gamma_0) \Omega} \\ 0 & 0 & \frac{a_0 b_0 \sin(\gamma_0)}{\Omega} \end{bmatrix} \quad (7)$$

1.3 Rotation matrix associated with twinning

The orientation relationship between twin and matrix is related by the rotation around a specific axis. The rotation matrix R for a rotation around axis $\mathbf{u} = (u_x, u_y, u_z)$ by an angle θ is:

$$R(\mathbf{u}, \theta) = \begin{bmatrix} \cos \theta + u_x^2 (1 - \cos \theta) & u_x u_y (1 - \cos \theta) - u_z \sin \theta & u_x u_z (1 - \cos \theta) + u_y \sin \theta \\ u_y u_x (1 - \cos \theta) + u_z \sin \theta & \cos \theta + u_y^2 (1 - \cos \theta) & u_y u_z (1 - \cos \theta) - u_x \sin \theta \\ u_z u_x (1 - \cos \theta) - u_y \sin \theta & u_z u_y (1 - \cos \theta) + u_x \sin \theta & \cos \theta + u_z^2 (1 - \cos \theta) \end{bmatrix} \quad (8)$$

By applying the matrix on the vector $[xyz]$, one can obtain the rotated vector $[x_r y_r z_r]$.

$$[x_r y_r z_r] = [xyz] R(\mathbf{u}, \theta) \quad (9)$$

This rotation matrix can be applied to the basis vectors, so that a crystal direction in the twin can be transformed into one in the matrix. For example, a crystal direction $[uvw]_T$ in the twin can be converted to a crystal direction in the matrix, $[uvw]_M$.

$$[uvw]_M = [uvw]_T (AR_T) (AR_M)^{-1} \quad (10)$$

R_T and R_M are the rotation matrices imposed on the twin and the matrix, respectively. In this equation, the crystal direction $[uvw]_T$ was converted to a vector in Cartesian coordinates by (AR_T) and transformed to

crystal direction in matrix by $(AR_M)^{-1}$. In a similar way, the cross product can be calculated in Cartesian coordinates and converted to fractional coordinates.

1.4 Calculation of angles

a) The angle θ between two vectors $[u_1v_1w_1]$ and $[u_2v_2w_2]$ is

$$\theta = \arccos \left(\frac{\left((u_1 u_2 a_0^2 + v_1 v_2 b_0^2 + w_1 w_2 c_0^2 + \cos(\gamma_0) (u_1 v_2 + u_2 v_1) a_0 b_0 + \cos(\beta_0) (u_1 w_2 + u_2 w_1) a_0 c_0 + \cos(\alpha_0) (v_1 w_2 + v_2 w_1) b_0 c_0) \right)}{I_{u_1v_1w_1} I_{u_2v_2w_2}} \right) \quad (11)$$

$$I_{uvw} = \sqrt{a_0^2 u^2 + b_0^2 v^2 + c_0^2 w^2 + 2 \cos(\gamma_0) a_0 b_0 u v + 2 \cos(\beta_0) a_0 c_0 u w + 2 \cos(\alpha_0) b_0 c_0 v w}$$

b) The angle θ between two crystal planes $(h_1k_1l_1)$ and $(h_2k_2l_2)$ is

$$\theta = \arccos \left(d_1 d_2 \left(\frac{S_{12} (h_1 k_2 + h_2 k_1) + S_{13} (h_1 l_2 + h_2 l_1) + S_{23} (k_1 l_2 + k_2 l_1) + S_{11} h_1 h_2 + S_{22} k_1 k_2 + S_{33} l_1 l_2}{\Omega^2} \right) \right) \quad (12)$$

where $\frac{1}{d^2} = (S_{11} h^2 + S_{22} k^2 + S_{33} l^2 + 2 S_{12} h k + 2 S_{13} h l + 2 S_{23} k l) / \Omega^2$.

$$S_{11} = b_0^2 c_0^2 \sin(\alpha_0)^2$$

$$S_{22} = a_0^2 c_0^2 \sin(\beta_0)^2$$

$$S_{33} = a_0^2 b_0^2 \sin(\gamma_0)^2$$

$$S_{12} = a_0 b_0 c_0^2 (\cos(\alpha_0) \cos(\beta_0) - \cos(\gamma_0))$$

$$S_{23} = a_0^2 b_0 c_0 (\cos(\alpha_0) \cos(\beta_0) - \cos(\gamma_0))$$

$$S_{13} = a_0 b_0^2 c_0 (\cos(\alpha_0) \cos(\beta_0) - \cos(\gamma_0))$$

The angle θ between two crystal directions $[u_1v_1w_1]$ and $[u_2v_2w_2]$ can be expressed by

$$\theta = \arccos \left(\frac{([u_1v_1w_1]A) \cdot ([u_2v_2w_2]A)}{(|[u_1v_1w_1]A| \cdot |[u_2v_2w_2]A|)} \right) \quad (13)$$

c) For the angle between two planes or between a direction and a plane, the matrix B is substituted for matrix A.

2. Selection of step height and complementary Burgers vectors.

In the text, we mention the selection of \mathbf{b} and h . An example with many choices is the $\Sigma 11$ (001) twin in *fcc* crystals [1]. The favored choice theoretically was $h = 4h_0$ because of its small Burgers vector and this agreed with experimental observation [2]. Another aspect is that there are symmetry related limitations on α . For the $\Sigma 11$ twin, the upper limit is 45° . For large angles a different $\{100\}$ variant with an angle reduced by 45° is selected. For a given DP there is a dichotomy in the choice of \mathbf{b}_g when there

is 2D coincidence of a boundary as for coherent twin planes [3, 4] and some grain boundaries [5]. If the repeat distance parallel to \mathbf{b}_g is \mathbf{a} , then the same twin can be created by an opposite sign complementary dislocation $-\mathbf{b}_{cg}$, where, for the same h

$$\mathbf{b}_g + \mathbf{b}_{cg} = \mathbf{a} \quad (14)$$

Thus, there is another limit. For the $\Sigma 11$ case \mathbf{b}_g is the appropriate choice when $\alpha < 22.5^\circ$, but for larger angles \mathbf{b}_{cg} is appropriate. Hence the limit for α is $\pm 22.5^\circ$.

For type I twins or type II precursors with the same h , both vectors have the same rational origin for the related \mathbf{t} vectors, and both have an associated but different twin angle α or α_c , in accord with the $2'$, m' symmetry, so the choice between them is obvious. An issue arises when there are different step heights. An example is Figure 2(b). For $h = 2h_0$, the \mathbf{t} vectors are symmetric, the origin is rational \mathbf{b}_g is small, and \mathbf{b}_{cg} is large. The choice of \mathbf{b}_g is obvious. For $h = h_0$, \mathbf{b}_g is large and \mathbf{b}_{cg} is the appropriate TD vector. However, the symmetric origin for \mathbf{b}_{cg} is irrational and would greatly complicate the TM analysis. Hence the unit TDs have Burgers vectors $\mathbf{b}_{cg} = (1/2) 2\mathbf{b}_g$, $h = 2h_0$ is selected for analysis.

References

1. R.J. Kurtz, R.G. Hoagland, J.P. Hirth JP. Computer simulation of extrinsic grain- boundary defects in the Sigma 11, $\langle 101 \rangle \{131\}$ symmetric tilt boundary. Phil. Mag. 79 (1999) 683-703.
2. K.L. Merkle, L.J. Thompson, F. Phillipp F. Thermally activated step motion observed by high-resolution electron microscopy at a (113) symmetric tilt grain-boundary in aluminum. Phil. Mag. Lett. 82 (2002) 589-597.
3. J. P. Hirth and R. W. Balluffi, On Grain Boundary Dislocations and Ledges, Acta Metall. 21 (1973) 929-42.
4. P.M. Anderson, J.P. Hirth, J. Lothe, Theory of dislocations, 3rd Ed., Cambridge (2017).
5. J.W. Cahn, Y. Mishin, A. Susuki. Duality of dislocation content of grain boundaries, Phil. Mag. 86 (2006) 3965-3980.